The protease activity of transthyretin reverses the effect of pH on the amyloid-β protein/heparan sulfate proteoglycan interaction: A biochromatographic study

ARTICLE *in* JOURNAL OF PHARMACEUTICAL AND BIOMEDICAL ANALYSIS · MAY 2014

Impact Factor: 2.98 · DOI: 10.1016/j.jpba.2014.04.021 · Source: PubMed

6 AUTHORS, INCLUDING:

Ambre Geneste
University of Franche-Comté
4 PUBLICATIONS **28** CITATIONS

SEE PROFILE

Lydie Lethier
University of Franche-Comté
9 PUBLICATIONS **9** CITATIONS

SEE PROFILE

Journal of Pharmaceutical and Biomedical Analysis 97 (2014) 88–96

Contents lists available at ScienceDirect

Journal of Pharmaceutical and Biomedical Analysis

journal homepage: www.elsevier.com/locate/jpba

The protease activity of transthyretin reverses the effect of pH on the amyloid-β protein/heparan sulfate proteoglycan interaction: A biochromatographic study

Ambre Geneste[a], Yves Claude Guillaume[a,c,*], Nadine Magy-Bertrand[a,b], Lydie Lethier[a], T. Gharbi[a], Claire André[a]

[a] Université de Franche-Comté, UFR SMP, EA 4662, Nanomedecine, Imagery Therapeupic Lab, Pôle Chimie Analytique Bioanalytique et Physique, 25030 Besançon cedex, France
[b] Département de Médecine Interne, CHRU Besançon, 25030 Besançon cedex, France
[c] Pôle Pharmaceutique, CHRU Besançon, 25030 Besançon cedex, France

ARTICLE INFO

Article history:
Received 6 February 2014
Received in revised form 18 April 2014
Accepted 21 April 2014
Available online 2 May 2014

Keywords:
Transthyretin
pH effect
Heparan sulfate proteoglycan.

ABSTRACT

Patients suffering of Alzheimer's disease (AD) are characterized by a low transthyretin (TTR) level in the brain. The effect of pH and TTR concentration in the medium on the β-amyloid protein (Aβ)/heparan sulfate proteoglycan (HSPG) association mechanism were studied using a biochromatographic approach. For this purpose, HSPG was immobilized via amino groups onto the amino propyl silica pre-packed column, activated with glutaraldehyde, by using the Schiff base method. Using an equilibrium perturbation method, it was clearly shown that Aβ can be bound with HSPG. This approach allowed the determination of the thermodynamic data of this binding mechanism. The role of the pH was also analyzed. Results from enthalpy–entropy compensation and the plot of the number of protons exchanged versus pH showed that the binding mechanism was dependent on pH with a critical value at pH = 6.5. This value agreed with a histidine protonation as an imidazolium cation. Moreover, the corresponding thermodynamical data showed that at pH > 6.5, van der Waals and hydrogen bonds due to aromatic amino acids as tyrosine or phenylalanine present in the N-terminal (N_T) part governed the Aβ/HSPG association. Aβ remained in its physiological structure in a random coil form (i.e. the non-amyloidogenic structure) because van der Waals interactions and hydrogen bonds were preponderant. At acidic pH (pH < 6.5), ionic and hydrophobic interactions, created by histidine protonation and hydrophobic amino acids, appeared in the Aβ/HSPG binding. These hydrophobic and ionic interactions led to the conversion of the random coil form of Aβ into a β-sheet structure which was the amyloidogenic folding. When TTR was incubated with Aβ, the Aβ/HSPG association mechanism was enthalpy driven at all pH values. The affinity of Aβ for HSPG decreased when TTR concentration increased due to the complexation of Aβ with TTR. Also, the decrease of the peak area with the increase of TTR concentration demonstrated that this Aβ/TTR association led to the cleavage of Aβ full length to a smaller fragment. For acidic pH (pH < 6.5), it was shown that the importance of the hydrophobic and ionic interactions decreased when TTR concentration increased. This result confirmed that Aβ was cleaved by TTR in a part containing only the N_T part. Our results demonstrated clearly that TTR reversed the effect of acidic pH and thus played a protective role in AD.

1. Introduction

Alzheimer's disease (AD) is one of the major causes of dementia and death among the elderly (Hardy et al., 1992). In this pathology, brains are characterized by neurofibrillary tangles and the presence of senile plaques (SPs). SPs primarily consist of amyloid β protein (Aβ). Aβ is a 4 kDa protein with two common isoforms, Aβ(1–40) (which is the major Aβ sequence ≈90% found circulating

* Corresponding author at: Pôle Pharmaceutique, CHRU Besançon, 25030 Besançon cedex, France. Tel.: +33 3 81 66 55 44; fax: +33 3 81 66 56 55.
E-mail address: yves.guillaume@univ-fcomte.fr (Y.C. Guillaume).

http://dx.doi.org/10.1016/j.jpba.2014.04.021
0731-7085/

in cerebrospinal fluid CSF) [1] and Aβ(1–42) [2] generated from the proteolytic cleavage of a large transmembrane glycoprotein, amyloid β precursor protein (APP). Hardy and Higgins [3] and Hardy and Selkoe [4] hypothesized that the deposition of Aβ is the causative agent of AD and neurofibrillary tangles, cell loss, vascular damage, and dementia as a direct result of the deposition, which is known as the "amyloid cascade hypothesis". As Aβ has a high propensity to form aggregated β-sheet [5] protein deposits in the SPs, AD is considered as the most common form of amyloidoses in the brain. Structurally, two domains in Aβ can be distinguished: a hydrophilic N-terminal (N_T) region with residues 1–28 and a hydrophobic C-terminal (C_T) region with residues 29–40, which always exists as a β-sheet, independently of the pH and the temperature. The structure of the N_T region depends on the type of interactions involved. Zhang et al. [6] showed that the stabilization of the random coil conformation was due to van der Walls bonds [7], and the β-sheet structure is formed by hydrophobic and ionic interactions [8,9]. It is well-known that extrinsic or environmental factors, such as the pH, influence the relative proportions of the random coil, α-helix and β-sheet solution structures and modulate the aggregation of the Aβ peptide into amyloid. The relative proportions of these structures and the fibrillogenesis are highly pH-dependent [5]; pH greatly influences the conformation of the first 28 amino acids. This segment unfolds into a random-coil conformation between pH 1–4 and above pH 7. Between pH 4 and 7, Soto et al. [5] demonstrated that it rapidly precipitates into an oligomeric β-sheet structure. The structure of the N_T region determines the beginning of the fibrillogenesis. Physiologically, Aβ is probably degraded as a physiological event in the endosomal/lysosomal pathway, where the pH is below 4 in the lysosomes and below 6.5 in the endosomes [10]. Moreover, acidosis in the brain, where the pH value is under 6.6, is correlated with AD [11]. As in many amyloidoses, several other proteins with the ability to modulate amyloid fibril formation accumulate in SPs, particularly heparan sulfate proteoglycan (HSPG) [12], which has been found to be associated with all amyloid deposits. HSPG is a biologic macromolecule characterized by a core protein to which glycosaminoglycan side-chains (GAG) are covalently attached. The main role of HSPG is still unknown but it seems to be a scaffold for amyloid fibril formation. Although, due to the sulfur group of HSPG, electrostatic interactions contribute a great amount of the binding energy, hydrogen-bonding, van der Waal interactions, and hydrophobic effects are also involved in the interactions with proteins [13]. It has been reported that Aβ is sequestrated by extracellular proteins present in CSF as apolipoprotein E, apolipoprotein J, and APP [14]. Furthermore, Schwarzman et al. [15] demonstrated that TTR could bind to Aβ and they hypothesized that TTR sequestrated Aβ in CSF and plasma, therefore preventing amyloid fibril formation and deposition. TTR is a thyroxin and retinol protein transporter, which is located in both serum and CSF. In serum, TTR can lead to transthyretin amyloidoses. However, in the brain, its role is undefined. Studies have shown that the TTR level in the brain is correlated with the presence of SPs. The TTR level decreases with the SP growth [16].

In order to understand the role of the TTR in the Aβ-aggregation, the effect of pH and different concentrations of TTR in the medium on the Aβ(1–40)/HSPG association was analyzed using a biochromatographic approach.

2. Materials and methods

2.1. Reagents

Heparan sulfate proteoglycan (HSPG), isolated from basement membrane of Engelbreth-Holm-Swarm mouse sarcoma, and transthyretin from human plasma were obtained from Sigma-Aldrich (Paris, France). Amyloid β protein: the Aβ(1–40) isoform was purchased from Abcam (London, England). Potassium dihydrogen phosphate and dipotassium hydrogen phosphate, used for the preparation of the mobile phases, were of analytical grade and purchased from Merck (Paris, France).

2.2. Apparatus

The HPLC system consisted of a Shimadzu LC-10ATvp pump (Champs-sur-Marne, France), a Rheodyne 7725 injection valve (Cotati, CA, USA) fitted with a 20 μL sample loop, and a Shimadzu SPD-10A UV–vis detector (Noisiel, France). The Silice Uptisphere® 120 Å 3 μm NH_2 column (50 mm × 4.6 mm column size) was furnished by Interchim (Montluçon, France). The preparation of the heparan sulfate proteoglycan column via the in situ technique is described below. Throughout the study, a constant flow-rate of 0.3 mL/min was maintained and the temperature varied between 10 and 40 °C.

2.3. Covalent immobilization technique of HSPG on silica-NH_2 particles

The "*in situ*" immobilization technique to prepare this new HSPG column was previously used by our group [17] for the immobilization of acetylcholinesterase on an ethylenediamine (EDA) monolithic convective interaction media (CIM) disk. The immobilization of HSPG, via the amino groups of the protein, onto the amino propyl silica pre-packed column, activated with glutaraldehyde, by using the Schiff base method, was thus carried out as follows. Firstly, the column was washed with phosphate buffer saline (PBS) (pH 6.5, 0.01 M) for 30 min at a flow-rate of 0.5 mL/min. Then, the silica-NH_2 particles were activated by recycling 10% of glutaraldehyde in PBS (pH 6.5, 0.01 M) for 10 h at the same flow-rate, followed by washing with PBS (pH 6.5, 0.01 M) during 1 h. 0.2 mg of HSPG was dissolved in 50 mL of PBS (pH 7.4, 0.01 M) and the protein solution continuously circulated through the column at a flow-rate of 0.3 mL/min for at least 24 h. The column was then injected with PBS (pH 7.4, 0.01 M) for 1 h and 0.1 M of sodium cyanoborohydride in 100 mL PBS (pH 7.4, 0.01 M) circulated during 5 h for reductive amination. The column was then washed with PBS (pH 7.4, 0.01 M) for 1 h and a solution of 0.2 M ethanolamine was injected for 3 h to deactivate the aldehyde groups. To finish, 0.1% of sodium azide circulated during 1 h for column conservation purposes.

The total mass of HSPG (192 μg) in the column was determined by elemental analysis. For this analysis, four fractions of the stationary phase were removed from the head to the end of the column. The maximum relative difference of the amount of immobilized HSPG between these different measurements was always 0.5%, therefore providing a homogeneous HSPG distribution in the column from the ends to the center.

2.4. Aβ incubation with TTR and chromatographic operating conditions

The effect of different concentrations of TTR on Aβ/HSPG binding was determined by using the experimental method described below. Aβ, at a concentration of 20 μM, was incubated at room temperature during 3 h with different concentrations of TTR (x) (x = 0, 2, 5, 10, 15 μM). 20 μL of Aβ + x in PBS 0.01 M at pH = 7.4 were injected and the resulting retention factor was determined at seven temperatures, i.e. 283, 288, 293, 298, 303, 308 and 313 K. 20 μL of TTR, at a concentration of 20 μM, were also injected in the chromatographic system in similar conditions. The mobile phase consisted of a phosphate buffer saline (0.01 M), which was prepared by mixing equimolar solutions of mono- and dibasic sodium phosphate to

produce the desired eluent pH adjusted to values equal to 7.4, 7, 6.5, 6, and 5.5. A total aqueous mobile phase was used so as to obtain a maximal retention of Aβ on the HSPG column. The experiments were carried out at a detection wavelength of 214 nm with a 10-nm bandwidth. The chromatographic system was left to equilibrate at each temperature for at least 1 h prior to each experiment.

2.5. Langmuir distribution isotherms

Aβ could tightly bind to the matrix of the column by using the HSPG stationary phase. The determination of the Langmuir distribution isotherms was described in a previous study for the analysis of specific binding sites of a series of acetylcholine esterase inhibitors on an acetylcholine esterase stationary phase [17]. For this purpose, the perturbation technique was used [18–21]. This method makes it possible to determine the adsorption isotherms by measuring the retention times of small sample sizes injected onto a column equilibrated with sample solutions at different concentration levels. In this work, the equilibration was carried out with 10 different concentrations of Aβ (0–20 μM) in the mobile phase used to obtain a stable detection. Then, 20 μL containing the most concentrated Aβ solution are injected onto the column. After the injection, the equilibrium condition is disturbed, the perturbation waves reach the column outlet, and a peak is recorded by the detector and its retention time is measured. Therefore, if Aβ is bound to two sites on the stationary phase, i.e. a specific site (site A with an adsorption constant, K_A, and a column saturation capacity, α_A) and second site, which is non-specific (site B with an adsorption constant, K_B, and a column saturation capacity, α_B), then the solute retention factor (k'), which is directly proportional to the slope of its adsorption isotherm, is given by the following equation:

$$k' = \frac{t - t_0}{t_0} = \phi \frac{dC_S}{dC_m} = \phi \left(\frac{\alpha_A K_A}{(1 + K_A C_m)^2} + \frac{\alpha_B K_B}{(1 + K_B C_m)^2} \right) \quad (1)$$

ϕ is the column phase ratio (volume of the stationary phase divided by the volume of the mobile phase), C_s and C_m are respectively the total concentration of Aβ in the stationary phase and that in the mobile phase. Eq. (1) was adapted to the solute retention factor, k', by a non-linear regression and the parameters $k'_A = \Phi K_A \alpha_A$ and $k'_B = \Phi K_B \alpha_B$ corresponding to the retention contributions of the two types of sites under linear conditions were calculated.

2.6. Van't Hoff plot of the Aβ-HSPG binding process

Valuable information about the processes driving the Aβ-HSPG association mechanism can be further gained by examining the temperature dependence of Aβ [22,23]. Under linear conditions, the temperature dependence of the retention factor is given by the following relationship:

$$\ln k' = \frac{-\Delta H^\circ + \Delta S^\circ}{RS} \quad (2)$$

where $\ln k' = f(1/T)$ is called van't Hoff plot.

In this equation, $\Delta S^{\circ *} = \Delta S^\circ / R + \ln \varphi$, where R is the gas constant, T is the column temperature in Kelvin, φ is the column phase ratio and ΔH° and ΔS° are the solute enthalpy and entropy variations occurring during the transfer of Aβ from the bulk solvent to the HSPG surface, respectively. If the HSPG stationary phase, Aβ and solvent properties are temperature invariant, a linear van't Hoff plot is obtained and ΔH° and $\Delta S^{\circ *}$ can be calculated from the slope and intercept.

Table 1
Values of the retention contribution of the two types of sites, k'_A and k'_B, the retention factor k' ($k' = k'_A + k'_B$) (extrapolated at $C_m = 0$) and the non-linear regression coefficients, r^2 and F (Langmuir model; Lang), for Aβ, standard deviations are in parentheses.

Solute molecule	k'_A	k'_B	k'	r^2; F-Lang
Aβ	0.142 (0.028)	0.004 (0.001)	0.146 (0.007)	0.9996;7552

3. Results

3.1. Langmuir distribution isotherm results and column stability

As the immobilization of HSPG on a silica support could lead to non-specific interactions, there tention contributions of these two types of sites, i.e. k'_A and k'_B, were determined from Eq. (1) at pH = 7.4 and 298 K. For each Aβ molecule and for each solute concentration in the bulk solvent, the most concentrated sample was injected three times into the chromatographic system and its retention factor was determined (see 'Langmuir distribution isotherms' section). The variation coefficients of the k' values were <0.3%, therefore indicating a high reproducibility and a good stability of the chromatographic system. With a weighted non-linear regression (WNLIN) which was used in earlier chromatographic studies [24], the k' values at various Aβ concentrations in the mobile phase were fitted in Eq. (1). After the WNLIN procedure, the constants of Eq. (1) were used to estimate the k' values with the measured values at the different Aβ concentrations in the mobile phase. The slope of the curve representing the variation of the estimated retention factors (k') (Eq. (1)) versus the experimental values (0.9999; the ideal value is 1.0000) and r^2 (0.998) indicate that there is an excellent correlation between the predicted and experimental retention factors. The non-linear regression coefficient r^2 and the F value (from the Fisher test with a confidence level at 95%) [24] were determined. These values are shown in Table 1. The F value constitutes a more discriminating parameter than the r^2 value when assessing the significance of the model equation [24]. From the full regression model, a student t-test was used to provide the basis for the decision as to whether or not the model coefficients were significant. Results of the student's t-test show that no variable can be excluded from the model. These results showed that Eq. (1) accurately describes the association behavior of Aβ with HSPG. Furthermore, an important conclusion can be drawn from these data i.e. the interactions between Aβ with the matrix of the stationary phase were disregarded (the k'_A and k'_B values are given in Table 1 and $k_B \ll k_A$). This important result was confirmed by the fact that Aβ was not retained on the aminopropyl silica column (i.e. the commercial AP column) under similar chromatographic conditions. Therefore, the non-specific binding sites of the HSPG column could be negligible. In order to evaluate the column reproducibility, three columns were prepared under identical conditions as described above: the retention factors at pH 7.4 (standard deviations equal to 0.024 for Aβ) were obtained with Aβ (0.143). The mobile phase was a PBS (pH 7.4, 0.01 M) mixture with a flow-rate of 0.3 mL/min and a column temperature equal to 308 K. The results showed that the temperature was reliable and reproducible. In addition, the standard reproducibility of this column expressed as the retention time measured as a relative standard deviation was <5%. After half a year and more than 300 injections, the decrease of the retention factor values of the column was <1.2%. Further in this paper, the k' values of Aβ representing its retention on the HSPG stationary phase were thus determined for a sample concentration in the mobile phase equal to zero; i.e. $C_m = 0$.

Table 2
Values of the peak areas of Aβ with TTR (x = 0, 2, 5, 10 or 15 μM).

x (μM)	pH 5.5	pH 6	pH 6.5	pH 7	pH 7.4
0	2594295	2259050	2092899	2486154	2871451
2	1347617	1669877	1616071	1286884	1863466
5	1232481	1617110	1110924	1000000	1218179
10	225289	93965	1052514	101124	495148
15	78228	46730	51045	47443	52606

Table 3
Values of the parameters of the $\log k' = \log k'_0 + \lambda_1 pH + \lambda_2 pH^2$ plot for all x values at pH = 7.4 and T = 298 K.

x (μM)	0	2	5	10	15
$\log k'_0$	9.90	12.90	10.47	10.15	5.51
λ_1	−2.82	−3.81	−3.90	−3.03	−1.51
λ_2	0.22	0.29	0.24	0.23	0.11
r^2	0.88	0.90	0.97	0.95	0.91

3.2. pH and TTR concentration effects on the Aβ/HSPG association process

All the experiments were repeated at least three times and the variation coefficients of the k' values were all less than 5% for all pH and x values, therefore indicating a high reproducibility and good stability of the chromatographic systems.

The chromatograms showed that the retention times decreased with the increase of TTR concentration. An example is given in Fig. 1, which shows that the retention times for x = 0 μM and for x = 15 μM were respectively 13.551 min (k' = 4.80) and 7.129 min (k' = 2.98).

The plot of k' versus x was drawn for all pHs being studied. All the curves exhibited a similar variation with a quadratic function. For example, Fig. 2 represented k' versus x at pH = 5.5 and at 298 K with the following equation:

$$k' = 0.01x^2 - 0.44x + 6.28 \quad r^2 = 0.99 \tag{3}$$

The related peak areas (A) were also investigated. The peak areas, determined at all pHs being studied, are included in Table 2. The log A versus log x curve, plotted for all pH values, showed that the area decreased when the TTR concentration increased. The trends obtained from Fig. 3 were not linear and the following associated equations were provided as examples:

$$\text{At pH} = 7.4: \quad \log A = -1.42x^2 + 0.22x + 6.33 \quad r^2 = 0.96 \tag{4}$$

$$\text{At pH} = 5.5: \quad \log A = -1.31x^2 + 0.34x + 6.33 \quad r^2 = 0.96 \tag{5}$$

Valuable information about the processes driving the Aβ/HSPG association mechanism could be further gained by examining the pH dependence on the Aβ/HSPG association.

When the pH of the bulk solvent changed, a fuller description was essential, which explicitly maintained the conservation of mass of each species and took into account the binding of H^+ to HSPG, Aβ and the HSPG/Aβ complex:

$$\text{HSPG}(H^+)_A + A\beta(H^+)_B + n_H^+ \rightleftharpoons \text{HSPG}/A\beta(H^-)_C \tag{6}$$

where $n_{H+} = C - (A + B)$ was the number of protons linked to this Aβ binding reaction of HSPG.

n_{H+} could be calculated using the following equation [25]:

$$\frac{\partial \log k'}{\partial \text{pH}} = n_{H^+} \tag{7}$$

Fig. 4 reported all the data acquired on the variations of the retention factors of Aβ when the bulk solvent pH increased from 5.5 to 7.4. Looking at the experimental data, it was evident that the trend was not linear. This was highlighted by the following quadratic function:

$$\log k' = \log k'_0 + \lambda_1 pH + \lambda_2 pH^2 \tag{8}$$

where k'_0 is the retention factor extrapolated at pH = 0 and $\lambda_{1,2}$ were constants related to the structure of Aβ. A quadratic relationship was obtained for all the x values. These constants were determined from the non-linear log k' versus pH plot by using Eq. (8). The log k'_0, λ_1, λ_2 and r^2 values are given in Table 3 for all x values. The slope of the log k' versus pH curve, determined from Eq. (8), gave the number of protons, n_{H+}, involved in the binding process of Aβ/HSPG. Fig. 5 showed how the n_{H+} values increased linearly with the pH and was practically equal to zero at pH = 6.5 for all x values.

3.3. Thermodynamic data of the Aβ/HSPG association process

The retention factor of Aβ on HSPG was calculated over the entire pH range ($5.5 \le pH \le 7.4$) and x value range ($0\ \mu M \le x \le 15\ \mu M$) with column temperatures (283–313 K). The ln k' versus $1/T$ plot was determined from these retention factors

Table 4
Thermodynamic parameters of the Aβ/HSPG association with TTR (x = 0, 2, 5, 10, 15 μM) (ΔH° (kJ/mol), $\Delta S^{\circ *}$ (no unit)). RSD < 0.70.

x (μm)	pH 5.5		pH 6		pH 6.5		pH 7		pH 7.4	
	ΔH°	$\Delta S^{\circ *}$	ΔH°	$\Delta S^{\circ *}$	ΔH°	$\Delta S^{\circ *}$	ΔH°	$\Delta S^{\circ *}$	ΔH°	$\Delta S^{\circ *}$
0	−1.51	1.10	−4.00	−0.21	−10.83	−3.27	−14.90	−4.70	−16.30	−5.06
2	−3.17	0.41	−5.81	−0.99	−12.36	−4.06	−13.64	−4.33	−18.47	−6.00
5	−4.39	−0.28	−4.63	−0.75	−11.13	−3.61	−13.64	−4.83	−15.15	−4.80
10	−4.30	−0.53	−5.06	−0.97	−11.14	−3.71	−13.51	−3.65	−15.58	−4.98
15	−7.70	−2.04	−7.97	−2,33	−12.49	−4.53	−11.10	−5.69	−15.48	−6.21

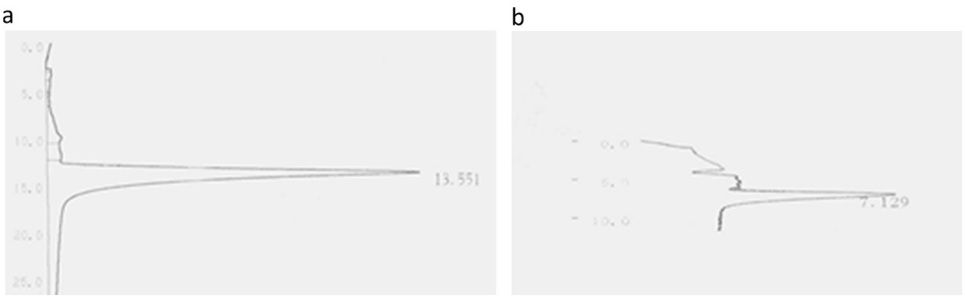

Fig. 1. Chromatograms at pH = 7.4 and T = 298 K of (a) Aβ without TTR, (b) Aβ + TTR (x = 15 μM).

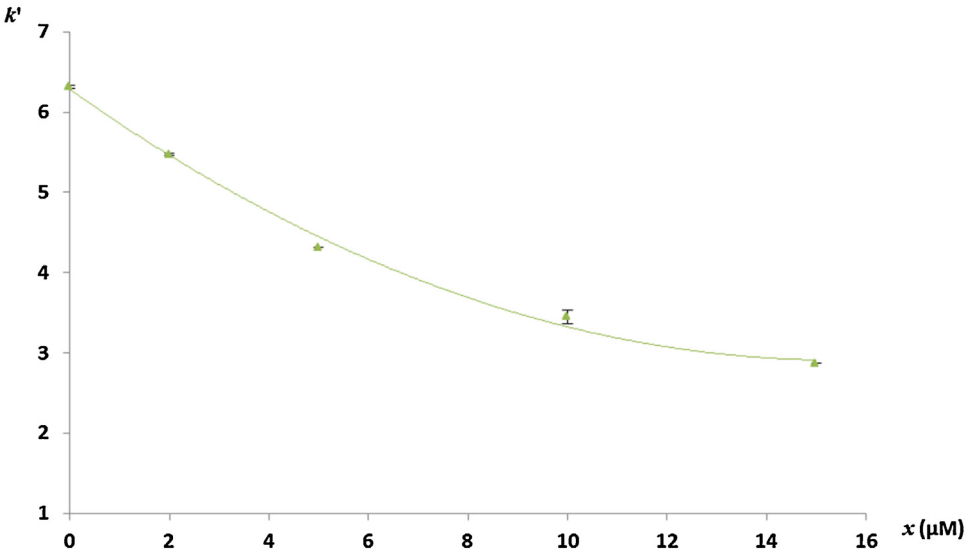

Fig. 2. k' versus x at pH = 5.5 and at 298 K.

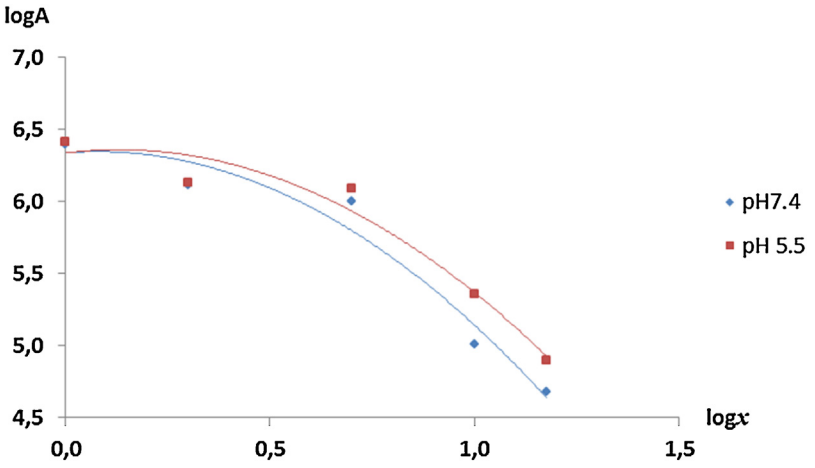

Fig. 3. log A versus log x at pH = 7.4 and pH = 5.5.

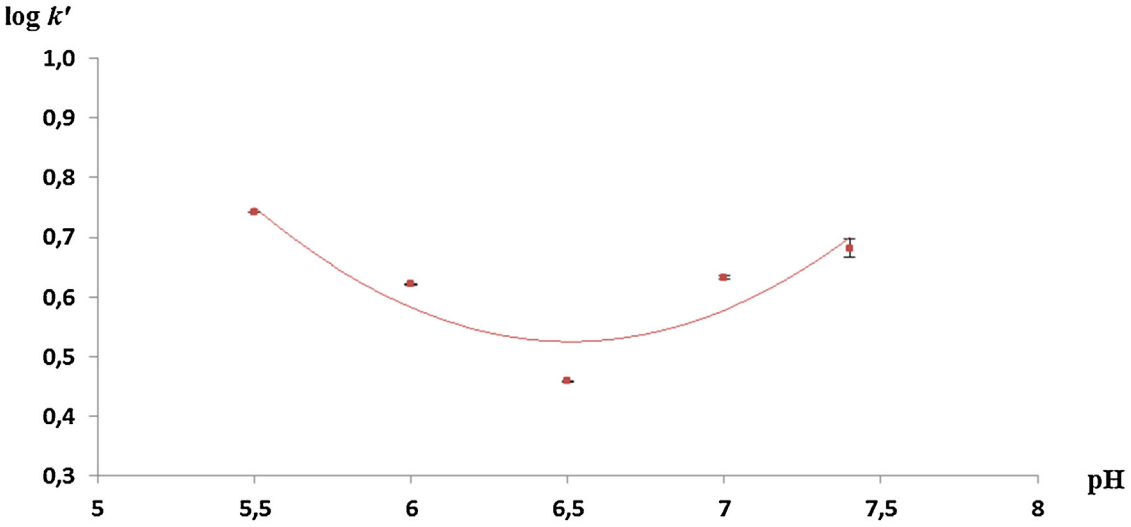

Fig. 4. log k' versus pH at 298 K.

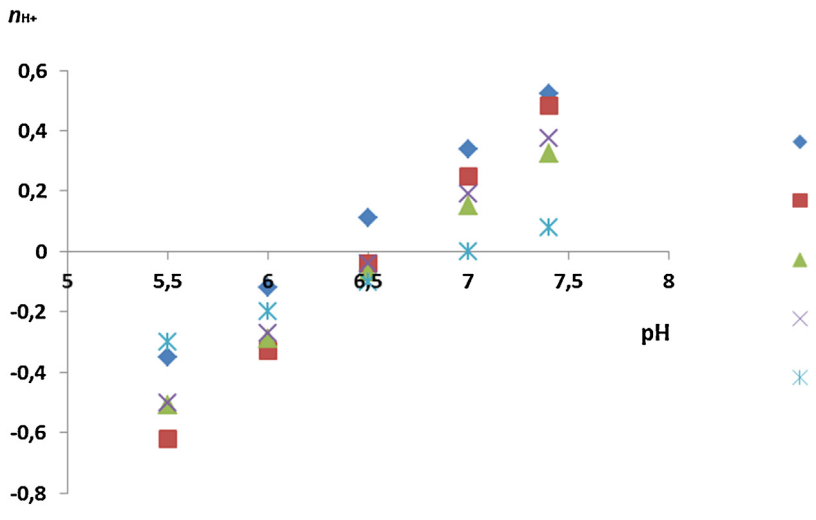

Fig. 5. pH dependence of the linked protons of Aβ with $x = 0$ (◆), 2 (■), 5 (▲), 10 (×), 15 μM (✳) at $T = 298$ K.

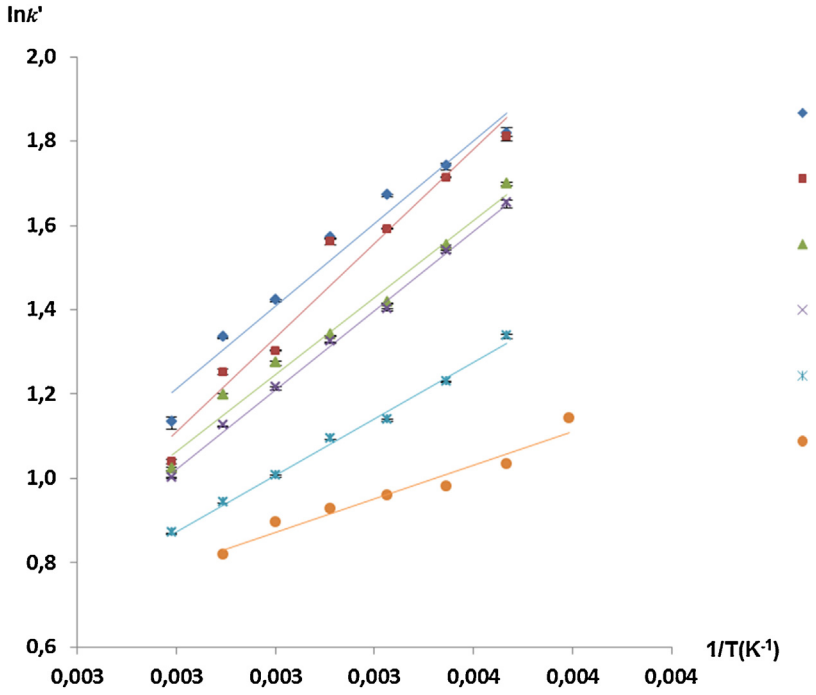

Fig. 6. van't Hoff plots of transthyretin (●) and of Aβ with $x = 0$ (◆), 2 (■), 5(▲), 10 (×), or 15 (✳) μM at pH = 7.4

for different pH values. Fig. 6 represents, for example, the van't Hoff plots at pH = 7.4 for all x values. These plots were all linear and the related correlation coefficients were in excess of 0.96.

The linear van't Hoff plots were used to calculate values of the thermodynamic parameters (ΔH° and $\Delta S^{\circ *}$). Table 4 provides the ΔH° and $\Delta S^{\circ *}$ values at all pH and x values.

A further thermodynamic approach to the analysis of a pH-dependent physicochemical process between Aβ, incubated with different TTR concentrations, and HSPG, was the enthalpy–entropy compensation [26], which is used in chromatographic procedures to analyze and compare the association or complexation mechanism for a group of compounds. Mathematically, the enthalpy–entropy compensation could be expressed by the following equation:

$$\ln k' = -\frac{\Delta H^\circ}{k}\left(\frac{1}{s} - \frac{1}{\beta}\right) - \frac{\Delta G^\circ_\beta}{k\beta} - \ln \phi \qquad (9)$$

ΔG°_β was the corresponding Gibbs free energy variation at the β compensation temperature. Fig. 7 shows the plot of $\ln k'$ (for $T = 298$ K) versus ΔH° for $x = 0$ μM. The plot presented a break at pH = 6.5 with two distinct domains, a (6.5–7.4) and b (5.5–6.5). The associated regression lines were:

$$\text{For domain a}: \quad \ln k' = -0.08\Delta \mathrm{H}^\circ + 0.13 \quad r^2 = 0.98 \qquad (10)$$

$$\text{For domain b}: \quad \ln k' = 0.07\Delta H^\circ + 1.76 \quad r^2 = 0.97 \qquad (11)$$

It appeared that the slopes were different and exhibited different β compensation temperatures: at 298 K, $\beta = 259$ K for domain a and $\beta = 398$ K for domain b. The break was also observed for all x values and the associated β compensation temperatures are indicated in Table 5.

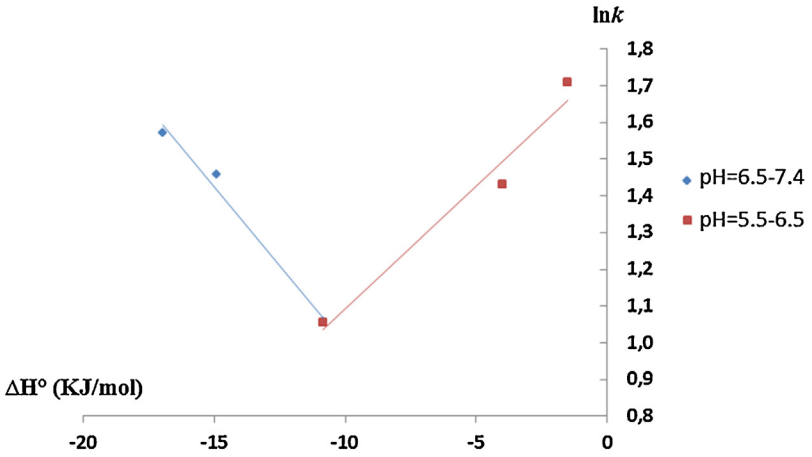

Fig. 7. Enthalpy–entropy compensation for Aβ at 298 K.

Table 5
Compensation temperatures of Aβ + x = 0, 2, 5, 10 and 15 μM.

x (μM)	β pH 6.5–7.4	β pH 5.5–6.5
0	259	398
2	251	402
5	259	401
10	263	444
15	251	456

4. Discussion

4.1. Association mechanism of Aβ/HSPG without TTR in the medium

The association mechanism of Aβ with HSPG without TTR in the medium (i.e. x = 0 μM) was analyzed at all pH values. Table 4 shows that the ΔH° values were always negative at all pH values, therefore demonstrating that van der Waals and hydrogen bonds played a major role in the Aβ/HSPG association mechanism. Aβ(1–40) included, in the 1–28 segment, aromatic amino acids such as one tyrosine at position 10 and three phenylalanines at positions 4, 19 and 20. Numerous studies have demonstrated that sulfate moieties of glycosaminoglycans were critical in Aβ interactions [27], the importance of the sulfate groups was already confirmed by a decrease in Aβ fibril formation in the presence of desulfated HS [28]. Van der Waals interactions could be explained by the interactions involving delocalized electrons from the aromatic ring systems of the Aβ aromatic amino acids with the sulfur atoms of HSPG. Also, interactions between aromatic amino acids themselves could induce van der Waals interactions, such as in APP interactions with HSPG [29].

However, the ln k' versus ΔH° plot (Fig. 7) presented a break at pH = 6.5 and the n_{H+} versus pH plot (Fig. 5) presented a positive n_{H+} value for pH > 6.5 and a negative n_{H+} value for pH < 6.5.

For pH > 6.5, when the pH increased, the ΔH° values decreased, therefore showing that van der Waals and hydrogen bonds were preponderant in the association mechanism and were involved at the complex interface forming a strong Aβ/HSPG hydrogen bond network. The hydrogen bond formation was confirmed by positive n_{H+} values showing that protons were taken up upon binding, which meant that a residue of the HSPG surface or of the Aβ molecule had increased its pK_a. The imidazole sidechain of the Histidine (His) residue had a pK_a of around 6. The imidazole polar hydrogen atom, which was a hydrogen-bond donor, could form a hydrogen bond interaction with amino acids from the core protein of HSPG.

Therefore, the van der Waals interactions mainly maintained the N_T part of Aβ(1–40) as a random coil, which was the physiological structure.

For pH < 6.5, when the pH decreased, ΔH° and $\Delta S^{\circ *}$ values strongly increased, and for pH < 5.5, $\Delta S^{\circ *}$ had a positive value ($\Delta H^{\circ}_{pH7.4} = -16.3$ kJ/mol and $\Delta S^{\circ *}_{pH7.4} = -5.06$, $\Delta H^{\circ}_{pH5.5} = -1.51$ kJ/mol and $\Delta S^{\circ *}_{pH5.5} = 1.10$). This result demonstrated that ionic and hydrophobic interactions appeared in the Aβ/HSPG association mechanism. The interactions between ionic species and hydrophobic interactions in an aqueous solution were characterized by small positive enthalpy variations and positive entropy variations [27]. Aβ possessed 3 His residues in the 14 first amino acids at positions 6, 13 and 14. The ionic interactions might be due to the protonation of His residues. The basic nitrogen atom on the protonated imidazole ring could have interacted with the negative charges (sulfur groups) of HSPG and with the amino acids from the core protein of HSPG [29]. This fact was corroborated by negative n_{H+} values (Fig. 5). This result confirmed McLaurin's study [28], which showed that residues 13–16 (His-His-Gln-Lys) of Aβ were considered critical for GAG interactions because their interactions with the sulfur atoms of HSPG were inhibited at pH values higher than 7 [30]. The hydrophobic interactions could be due to hydrophobic amino acids, which have interacted with the core part of the HSPG. Aβ possessed 11 hydrophobic amino acids in the N_T part, such as leucine (Leu) 17 and valine (Val) 18. Furthermore, studies have showed that these two amino acids were involved in hydrophobic interactions and were often found in proteins with a β-sheet structure [31]. Moreover, studies have suggested that the presence of amino acids with a high propensity for a β-sheet secondary structure in a sequence, that is otherwise designed for a α-helical character, made the second structural motif possible [32]. Therefore, the hydrophobic and ionic interactions added to the β-sheet conformation of the C_T part were responsible for the conformational change of the N_T part of Aβ into a β-sheet structure.

Our results have clearly demonstrated the role played by pH in the conversion of the random coil form of Aβ into a β-sheet structure, which is the amyloidogenic folding.

4.2. Effect of transthyretin on Aβ/HSPG association

Figs. 1 and 2, respectively show that both the retention time and thus the retention factor decreased with the increase of TTR concentrations. These results have demonstrated that the presence of TTR decreased the affinity of Aβ for HSPG due to the association of Aβ with TTR in the medium [15]. This decrease was observed at all pH values. The Aβ/TTR complex did not interact with HSPG.

Table 2 and Fig. 3 indicate that the peak area decreased when the TTR concentration increased at all pH values. These results were due to the proteolytic activity of TTR. Proteolytic activity was assigned to TTR as a cerebral physiological function [33].

According to Table 4, for pH > 6.5, there were no significant differences in the values of the thermodynamic data at all TTR concentrations (at pH = 7.4: $\Delta H^{\circ}_{A\beta+x=0\,\mu M} = -16.3$ kJ/mol, $\Delta S^{\circ *}_{A\beta+x=0\,\mu M} = -5.06$ and $\Delta H^{\circ}_{A\beta+x=15\,\mu M} = -15.48$ kJ/mol, $\Delta S^{\circ *}_{A\beta+x=15\,\mu M} = -6.21$). These data demonstrated that van der Waals and hydrogen bonds were preponderant in the association process. Therefore, Aβ remained in a random coil form, which was not the amyloidogenic structure.

For pH < 6.5, the decrease of the thermodynamic values with the TTR concentration (at pH = 5.5: $\Delta H^{\circ}_{A\beta+x=15\,\mu M} = -1.51$ kJ/mol and $\Delta S^{\circ *}_{A\beta+x=0\,\mu M} = 1.10$, $\Delta H^{\circ}_{A\beta+x=15\,\mu M} = -7.70$ kJ/mol and $\Delta S^{\circ *}_{A\beta+x=15\,\mu M} = -2.04$) demonstrated that the predominance of the hydrophobic and ionic interactions decreased as the TTR concentration increased. These results showed that the hydrophobic amino acids and/or the His residues were less involved in the binding when TTR concentration increased. These results confirmed the cleavage of Aβ by TTR. In addition, Costa et al. [34] showed that TTR cleaved the Aβ peptide after 3 h of incubation into one segment of 1698 Da corresponding to 1–14 amino acids. Thus, this cleavage removed a big part of Aβ with the C_T part included. Therefore, the higher the concentration of TTR incubated with Aβ, the greater the amount of cleaved Aβ. The level of Aβ in its entire length corresponding to free Aβ decreased. Residues 13–16, critical for GAG interactions, and many hydrophobic residues, such as Val18 and Leu17, responsible for hydrophobic interactions, were almost all removed during the cleavage; the importance of hydrophobic and ionic interactions in the association mechanism was therefore reduced [35]. The Aβ fragment remained in a random coil form and did not aggregate with HSPG.

5. Conclusion

For the first time, a new biochromatographic column was developed to study the effect of pH and the TTR concentration (x) on the Aβ/heparan sulfate proteoglycan (HSPG) association mechanism. For this purpose, HSPG was immobilized via its amino groups on a chromatographic support using an "*in situ*" immobilization technique. It was shown that the Aβ/HSPG binding mechanism was dependent on pH and x. For pH > 6.5 and for all TTR concentrations being studied, van der Waals and hydrogen bonds were preponderant in the Aβ/HSPG binding process and the N_T part of Aβ was stabilized in a random coil form. For acidic pH values (pH < 6.5), the effect of pH was dependent on TTR concentrations: (i) for $x = 0$ μM (i.e. without TTR), ionic and hydrophobic interactions (due to residues such as His, Leu and Val) appeared and were responsible for the random coil → β-sheet conversion, (ii) for $2\,\mu M \leq x \leq 15\,\mu M$ and all pH values, the affinity of Aβ for HSPG and the peak area decreased as the TTR concentration increased, therefore demonstrating a complex formation between Aβ and TTR, followed by a cleavage of Aβ by TTR. Moreover, at pH < 6.5, the importance of the ionic and hydrophobic interactions decreased with the increase of the TTR concentration. So, when the TTR concentration increased, the conversion of the random coil form of Aβ into the β-sheet structure decreased. These results demonstrated that Aβ was cleaved by TTR in a small fragment containing only the N_T part, which remained in a random coil form and didn't form amyloidogenic deposits. Our results have clearly demonstrated that TTR reverses the effect of pH and therefore plays a protective role in Alzheimer's disease.

References

[1] M. Hashimoto, H. Md Shahdat, S. Yamashita, M. Katakura, Y. Tanabe, H. Fujiwara, S. Gamoh, T. Miyazawa, H. Arai, T. Shimada, O. Shido, DHA disrupts in vitro amyloid β1-40 fibrillation and concomitantly inhibits amyloid levels in cerebral cortex tissue of Alzheimer's disease model rats, J. Neurochem. 107 (2008) 1634–1646.

[2] D.B. Teplow, Structural and kinetic features of amyloid β-protein fibrillogenesis, Amyloid 5 (1998) 121–142.

[3] J.A. Hardy, G.A. Higgins, Alzheimer's disease: the amyloid cascade hypothesis, Science 256 (1992) 184–185.

[4] J. Hardy, D.J. Selkoe, The amyloid hypothesis of Alzheimer's disease: progress and problems on the road to therapeutics, Science 297 (2002) 353–356.

[5] C. Soto, M.C. Brañes, J. Alvarez, N.C. Inestrosa, The alpha-helical to beta-strand transition in the amino-terminal fragment of the amyloid beta-peptide modulates amyloid formation, J. Neurochem. 63 (1994) 1191–1198.

[6] S. Zhang, K. Iwata, M.J. Lachenmann, J.W. Peng, S. Li, E.R. Stimson, Y.A. Lu, M. Felix, J.E. Maggio, J.P. Lee, The Alzheimer's peptide Aβ adopts a collapsed coil structure in water, J. Struct. Biol. 130 (2000) 130–141.

[7] K. Pagel, T. Vagt, B. koksch, Directing the secondary structure of polypeptides at will: from helices to amyloids and back again? Org. Biomol. Chem. 3 (2005) 3843–3850;
M. Almeida Liz, C.J. Faro, M.J. Saraiva, M. Mendes Sousa, Transthyretin, a new cryptic protease, J. Biol. Chem. 279 (2004) 21431–21438.

[8] S. Deechongkit, E.T. Powers, S.L. You, J.W. Kelly, Controlling the morphology of cross β-sheet assemblies by rational design, J. Am. Chem. Soc. 127 (2005) 8562–8570.

[9] H. Dong, D. Hartgerink, Role of hydrophobic clusters in the stability of α-helical coiled coils and their conversion to amyloid-like β-sheets, Biomacromolecules 8 (2007) 617–623.

[10] J. Li, T. Kanekiyo, M. Shinohara, Y. Zhang, M.J. LaDu, H. Xu, G. Bu, Differential regulation of amyloid-β endocytic trafficking and lysosomal degradation by apolipoprotein E isoforms, J. Biol. Chem. 287 (2012) 44593–44601.

[11] M. Pirchl, J. Marksteiner, C. Humpel, Effects of acidosis on brain capillary endothelial cells and cholinergic neurons: relevance to vascular dementia and Alzheimer's disease, Neurol. Res. 28 (2006) 657–664.

[12] A.D. Snow, H. Mar, D. Nochlin, K. Kimata, M. Sato, S. Suzuki, J. Hassell, T.N. Wight, The presence of heparan sulfate proteoglycans in the neuritic plaques and congophilic angiopathy in Alzheimer's disease, Am. J. Pathol. 133 (1988) 456–463.

[13] S. Sarrazin, W.C. Lamanna, J.D. Esko, Heparan sulfate proteoglycans, Cold Spring Harb. Perspect. Biol. (2011) 1–33.

[14] W.J. Strittmatter, K.H. Weisgraber, D.Y. Huang, L.M. Dong, G.S. Salvesen, M. Pericak-Vance, D. Schmechel, D.E. Saunders, A.M. Goldgaber, A.D. Roses, Binding of human apolipoprotein E to synthetic amyloid beta peptide: isoform-specific effects and implications for late-onset Alzheimer disease, Proc. Natl. Acad. Sci. U.S.A. 90 (1993) 8098–8102.

[15] A.L. Schwarzman, L. Gregori, M.P. Vitek, S. Lyubski, W.J. Strittmatter, J.J. Enghilde, R. Bhasin, J. Silverman, K.H. Weisgraber, P.K. Coyle, M.G. Zagorski, J. Talafous, M. Eisenberg, A.M. Saunders, A.D. Roses, D. Goldgaber, Transthyretin sequesters amyloid beta protein and prevents amyloid formation, Proc. Natl. Acad. Sci. U.S.A. 91 (1974) 8368–8372.

[16] E.M. Castano, A.E. Roher, C.L. Esh, T.A. Kokjohn, T. Beach, Comparative proteomics of cerebrospinal fluid in neuropathologically-confirmed Alzheimer's disease and non-demented elderly subjects, Neurol. Res. 28 (2006) 155–163.

[17] F. Ibrahim, Y.C. Guillaume, M. Thomassin, C. Andre, Magnesium effect on the acetylcholinesterase inhibition mechanism: a molecular chromatographic approach, Talanta 79 (2009) 804–809.

[18] J.F.K. Huber, R.G. Gerriste, Evaluation of dynamic gas chromatographic methods for the determination of adsorption and solution isotherms, J. Chromatogr. A 58 (1971) 137–141.

[19] C. Blumel, P. Hugo, A. Seidel Morgenstern, Quantification of single solute and competitive adsorption isotherms using a closed-loop perturbation method, J. Chromatogr. A 865 (1999) 51–71.

[20] P. Jandera, S. Berncekova, K. Mihlbachler, G. Guiochon, V. Backovska, J. Planeta, Fitting adsorption isotherms to the distribution data determined using packed micro-columns for high-performance liquid chromatography, J. Chromatogr. A 925 (2001) 19–29.

[21] C. André, Y.C. Guillaume, Reanalysis of chiral discrimination of phenoxypropionic acid herbicides on a teicoplanin phase using a Bi-langmuir approach, Chromatographia 58 (2003) 201–206.

[22] Y.C. Guillaume, C. Guinchard, Retention mechanism of weak polar solutes in reversed phase liquid chromatography, Anal. Chem. 68 (1996) 2869–2873.

[23] C. André, Y.C. Guillaume, Saccharose effects on surface association of phenol derivatives with porous graphitic carbon, J. Chromatogr. A 1029 (2004) 21–28.

[24] C. Andre, C. Guyon, Y.C. Guillaume, Rodenticide – humic acid adsorption and role of humic acid on their toxicity on human keratinocytes: chromatographic approach to support biological data, J. Chromatogr. B 813 (2004) 295–302.

[25] T. Bagnost, Y.C. Guillaume, M. Thomassin, J.F. Robert, A. Berthelot, A. Xicluma, C. Andre, Immobilization of arginase and its application in an enzymatic chromatographic column: thermodynamic studies of nor-NOHA/arginase binding and role of the reactive histidine residue, J. Chromatogr. B 856 (2007) 113–120.

[26] Y.C. Guillaume, E. Peyrin, A. Berthelot, Chromatographic study of magnesium and calcium binding to immobilized human serum albumin, J. Chromatogr. B 728 (1999) 167–174.

[27] G.M. Castillo, W. Lukito, T.N. Wigh, A.D. Snow, The sulfate moieties of glycosaminoglycans are critical for the enhancement of beta-amyloid protein fibril formation, J. Neurochem. 72 (1999) 1681–1687.
[28] J. McLaurin, T. Franklin, X.X. Zhang, J. Deng, P.E. Fraser, Interactions of Alzheimer amyloid-beta peptides with glycosaminoglycans effects on fibril nucleation and growth, Eur. J. Biochem. 266 (1999) 1101–1110.
[29] S. Narindrasorasak, D. Lowery, P. Gonzalez-Dewitt, T.A. Poorman, B. Greenberg, R. Kisilevsky, High affinity interactions between the Alzheimer's P-amyloid precursor proteins and the basement membrane form of heparan sulfate proteoglycan, J. Biol. Chem. 286 (1991) 12878–12883.
[30] C. Hilbich, B. Kisters-Woike, J. Reed, C. Masters, K. Beyreuther, Aggregation and secondary structure of synthetic amyloid beta A4 peptides of Alzheimer's disease, J. Mol. Biol. 218 (1991) 149–163.
[31] P.Y. Chou, G.D. Fasman, Prediction of the secondary structure of proteins from their amino acid sequence, Adv. Enzymol. Relat. Areas Mol. Biol. 47 (1978) 45–148.
[32] K. Pagel, S.C. Wagner, K. Samedov, H. von Berlepsch, C. Bottcher, B. Koksch, Random coils, β-sheet ribbons, and α-helical fibers: one peptide adopting three different secondary structures at will, J. Am. Chem. Soc. 128 (2006) 2196–2197.
[33] M. Almeida Liz, C.J. Faro, M.J. Saraiva, M. Mendes Sousa, Transthyretin: a new cryptic protease, J. Biol. Chem. 279 (2004) 21431–21438.
[34] R. Costa, A. Gonçalves, M.J. Saraiva, I. Cardoso, Transthyretin binding to A-beta peptide – impact on A-beta fibrillogenesis and toxicity, FEBS Lett. 582 (2008) 936–943.
[35] A. Geneste, Y. Guillaume, N. Magy-Bertrand, C. Andre, Effect of transthyretin and pH on Aβ(1–40)/heparan sulfate proteoglycan association, in: AAPS Symposium, 2013.